


DATASET BRIEF

Quantitative proteomic analyses reveal the impact of nitrogen starvation on the proteome of the model diatom *Phaeodactylum tricornutum*

Josselin Lupette^{1,2} | Marianne Tardif³ | Sabine Brugière³ | Yohann Couté³  |
 Juliette Salvaing¹ | Eric Maréchal¹ 

¹Laboratoire de Physiologie Cellulaire et Végétale, CEA, CNRS, INRAE, Université Grenoble Alpes, IRIG, CEA Grenoble, Grenoble, France

²Laboratoire de Biogenèse Membranaire, CNRS, Université de Bordeaux, Villenave d'Ornon, France

³Université Grenoble Alpes, INSERM, CEA, UMR BioSanté U1292, CNRS, CEA, FR2048, Grenoble, France

Correspondence

Juliette Salvaing and Eric Maréchal, Laboratoire de Physiologie Cellulaire et Végétale, CEA, CNRS, INRAE, Université Grenoble Alpes, IRIG, CEA Grenoble, 17 Avenue des Martyrs, 38000, Grenoble, France. Email: juliette.salvaing@cea.fr and eric.marechal@cea.fr

Funding information

Agence Nationale de la Recherche, Grant/Award Numbers: ANR-10-INBS-08-01, ANR-10-LABEX-04, ANR-15-IDEX-02, ANR-17-EURE-0003

Abstract

Diatoms are one of the largest groups in phytoplankton biodiversity. Understanding their response to nitrogen variations, present from micromolar to near-zero levels in oceans and fresh waters, is essential to comprehend their ecological success. Nitrogen starvation is used in biotechnological processes, to trigger the remodeling of carbon metabolism in the direction of fatty acids and triacylglycerol synthesis. We evaluated whole proteome changes in *Phaeodactylum tricornutum* after 7 days of cultivation with 5.5-mM nitrate (+N) or without any nitrogen source (–N). On a total of 3768 proteins detected in biological replicates, our analysis pointed to 384 differentially abundant proteins (DAP). Analysis of proteins of lower abundance in –N revealed an arrest of amino acid and protein syntheses, a remodeling of nitrogen metabolism, and a decrease of the proteasome abundance suggesting a decline in unselective whole-proteome decay. Analysis of proteins of higher abundance revealed the setting up of a general nitrogen scavenging system dependent on deaminases. The increase of a plastid palmitoyl-ACP desaturase appeared as a hallmark of carbon metabolism rewiring in the direction of fatty acid and triacylglycerol synthesis. This dataset is also valuable to select gene candidates for improved biotechnological properties.

KEYWORDS

diatom, nitrogen starvation, *Phaeodactylum*, proteome remodeling, quantitative proteomics

Diatoms are one of the largest groups of phytoplankton biodiversity, dominating oceanic and freshwater ecosystems [1]. They have attracted attention as a promising resource for multiple biotechnological applications [2–5]. In spite of their ecological importance and economic potential, efforts are still needed to advance knowledge on their unique metabolism and powerful acclimation to their changing environment. A major issue is to comprehend their response to the availability of nitrogen, which supply can vary from a high abundance in lakes, rivers, or coastal areas (in the micromolar to the lower millimolar range), to complete absence in open ocean or after its exhaustion

by living organisms [6]. This question is of further interest, as nitrogen starvation is also used in biotechnological processes as a mean to trigger a remodeling of carbon metabolism for lipid production.

The understanding of pennate diatom biology has benefited from developments on the model species, *Phaeodactylum tricornutum*, for which efforts have been made to sequence its genomes [7], and study transcriptional [8–15] and lipidomic responses [13, 16, 17] to a variety of environmental conditions. A few whole-cell and purified organelle proteomic analyses have been achieved [18–23]. Extensive studies of *P. tricornutum* response to a lack of nitrogen have been reported from

transcriptomics to metabolomics and lipidomics [16, 24]. A proteomic comparison of *P. tricornutum* acclimated to very high (37.5 mM NO₃⁻) and high (21.3 mM NO₃⁻) nitrate concentrations [25], did not account for the actual response to natural conditions in oceans, where nitrate is commonly found in the low micromolar to almost zero levels [6]. A proteomic study was performed on *P. tricornutum* grown in presence of 0.88 mM NO₃⁻, and 24 h after removal of nitrate [26], a timeframe too short to reflect all changes following transcriptomic reprogramming and protein turnover.

Here we used conditions established previously [16], with *P. tricornutum* cultivated for seven days in a nitrogen-replete medium called +N (containing 5.5 mM NO₃⁻), or a nitrogen-starved medium called -N (without any nitrogen) (Supplemental Methods). A mass spectrometry (MS)-based label-free quantitative proteomic analysis was conducted on whole-cell protein extracts (Supplemental Methods). To enhance the proteome coverage, peptides recovered from in-gel digestion were separated into four strong cation exchange (SCX) fractions before nanoLC-MS/MS data acquisitions. Identification and quantification of proteins were achieved by MaxQuant [27]. For identification, we used a *P. tricornutum* protein sequence database compiling the nuclear-encoded sequences (12,178 sequences) downloaded from Ensembl [28] and organellar-encoded sequences downloaded from NCBI (165 sequences). Four thousand four hundred and seventy-three proteins were identified (false discovery rates (FDRs) ≤1% at peptide-spectrum match and protein levels). The differential analysis of protein abundances was conducted using ProStaR [29] on the extracted intensity-based absolute quantification (iBAQ [30]) values. Data filtering was performed to keep only proteins reproducibly detected in the different replicates of one of the two conditions. This produced a set of 3768 proteins (Table S1), out of which 3226 were functionally annotated in the UniprotKB [31] (Table S2). Fourteen percent of proteins were not functionally annotated (no domain detection or gene ontology (GO) assessment, based on the UniprotKB standards), which is in the range of recent proteomic studies in *P. tricornutum* [21] (16%). After normalization of iBAQ values across samples and imputation of missing values, a statistical analysis was performed using limma. The differentially abundant proteins (DAP) were sorted out according to two criteria: fold change (FC) ratio between compared conditions of at least four (i.e., |Log2FC(N-/N+)| ≥ 2), and a limma *p*-value inferior to 0.004 (i.e., Log10(*p*-value) ≥ 2.4), allowing to reach a false discovery rate (FDR) below 1% according to the Benjamini-Hochberg estimator. With these criteria, 384 DAP were selected, including 142 more abundant and 242 less abundant proteins in the -N condition (Figure S1 and Table S3).

We analyzed the enrichment in GO and annotation terms using the DAVID functional annotation tool [32, 33] (Supplemental Methods). For this purpose, sequences with protein domains and/or GO terms recorded in UniprotKB [31] were used. Amongst the 142 DAP showing an increase in -N, 125 proteins were annotated with a Uniprot ID (Table S3). DAVID returned seven clusters with a GO or functional annotation enrichment compared to *P. tricornutum* CCAP 1055/1 full proteome. Four clusters were returned with an enrichment score higher than 1 (Table 1). 20 protein sequences were not

clustered. This analysis highlighted the increase of enzymes involved in a remodeling of the nitrogen metabolism, previously shown to be sensitive to the redox status upon N stress [34]. The increase in glutamate and glutamine synthases and urea transporter (Tables 1 and S1) argue for an upregulation of the ornithine urea cycle concomitantly with TAG accumulation, consistently with past studies in low N [35] or high nitric oxide conditions [13]. It also highlighted the increase of nuclear components and transcription factors, consistently with our current understanding of *P. tricornutum* reprogramming under phosphorus starvation [36].

Among the 242 DAP showing a decrease, 204 proteins could be annotated with a Uniprot ID. DAVID returned 17 clusters with an enrichment of GO or functional annotation terms. Eight clusters were returned with an enrichment score higher than 1 (Table 2). Fifty protein IDs were not clustered. This analysis highlighted the decrease of enzymes involved in amino acid, protein, and chlorophyll syntheses, as expected in a nitrogen-saving context. The abundance of quality control components (proteasome, autophagy) is decreased, suggesting that the mobilization of nitrogen from proteins does not involve general degradation systems and is likely highly selective.

We compared the DAP dataset with a study of the differential expression of mRNA between nitrogen-replete and nitrogen-starved conditions [24]. This transcriptomic study was performed 2 and 3 days after nitrogen removal from a medium containing 0.88-mM NO₃⁻. Although conditions are different, this early reprogramming of *P. tricornutum* gene expression is expected to contribute to a remodeling of the proteome in later stages, such as after 7 days of starvation.

Out of the 78 upregulated transcripts [24], 32 corresponded to proteins detected in this study. This may be explained by the different conditions in both studies. Most of the detected upregulated transcripts (59%) may also correspond to low-abundance proteins, proteins with lower tryptic-peptide yields, or proteins with changes in abundance lower than the levels retained. Thirty-one were annotated with a Uniprot ID (Table S4). Most of them (26 proteins) showed no apparent change in abundance, suggesting that the transcriptional upregulation may be either minor or counterbalanced by a regulation at the translational and/or post-translational levels, rescuing them from a degradation or rapid turnover. High transcript levels may not necessarily reflect in high protein levels. Only five upregulated transcripts corresponded to proteins with higher abundance in the present proteomic analysis:

- a committing step of plastid fatty acid synthesis, B7FQK1 (plastid acyl-acyl carrier protein (ACP) desaturase);
- five deamidases; B7FXR0, B7FYS6, and B7G3J7 (three formamidases); B7GBV8 (protein with a CMP/dCMP-type deaminase motif); and B7GE02 (with a deamidase motif).

The choreographed transcriptomic and proteomic response to a depletion of nitrogen seems, therefore, marked by the massive production of amidases involved in nitrogen scavenging and recycling, breaking down amides from nitrogen-rich metabolites, and releasing ammonium (NH₄⁺). It also highlights the onset of fatty acid synthesis.

TABLE 1 Analysis of 125 functionally annotated proteins, which abundance was significantly increased in *P. tricornutum* whole proteome in nitrogen-starved conditions

Annotation cluster 1	Enrichment score: 2.83	Count	P-value
GO term "cellular component"	Nucleus	11	7.0E−6
UP term "cellular component"	Nucleus	10	9.3E−5
GO term "molecular function"	Transcription factor activity,sequence-specific DNA binding	8	1.3E−4
INTERPRO	Heat shock factor (HSF)-type,DNA-binding	5	6.2E−3
UP sequence feature	DOMAIN:HSF_DOMAIN	5	8.6E−3
GO term "molecular function"	Sequence-specific DNA binding	5	1.3E−2
SMART	HSF	5	1.6E−2
UP keyword "molecular function"	DNA-binding	8	2.3E−2
Annotation cluster 2	Enrichment score: 2.5	Count	P-value
GO term "molecular function"	Transcription factor activity,sequence-specific DNA binding	8	1.3E−4
INTERPRO	Basic-leucine zipper domain	3	1.5E−2
UP sequence feature	DOMAIN:BZIP	3	1.6E−2
Annotation cluster 3	Enrichment score: 1.9	Count	P-value
KEGG pathway	Nitrogen metabolism	4	9.3E−4
KEGG pathway	Alanine, aspartate, and glutamate metabolism	4	3.6E−3
KEGG pathway	Arginine biosynthesis	3	2.8E−2
KEGG pathway	Biosynthesis of amino acids	4	2.7E−1
Annotation cluster 4	Enrichment score: 1.38	Count	P-value
UP sequence feature	DOMAIN:Fe2OG dioxygenase	4	9.6E−3
INTERPRO	Oxoglutarate/iron-dependent dioxygenase	4	1.5E−2
UP keyword "ligand"	Iron	6	5.4E−2
GO term "molecular function"	Metal ion binding	9	1.2E−1
UP keyword "ligand"	Metal-binding	11	1.3E−1

Analysis was performed using DAVID functional annotation tool [32, 33]. The GO terms and keywords from Uniprot (UP), INTERPRO, COG, and KEGG databases were clustered and the statistical significance of each cluster was assessed using an Enrichment score (Supplemental Methods). Functional annotation clusters were considered significant at enrichment score > 1 using the *Phaeodactylum tricornutum* proteome in UniprotKB as background.

The remarkable upregulation of the transcription (FC = 4.7) and protein level increase (FC = 5.8) of the plastid acyl-ACP desaturase is consistent with a recent study showing that the acyl-ACP desaturase was a controlling point of the flux of fatty acids exported from the plastid toward the production of triacylglycerol in the cytoplasm of *P. tricornutum* [37].

Out of the 248 downregulated genes [24], 176 (>70%) corresponded to proteins detected in our study. Amongst these, 170 were annotated with a Uniprot ID (Table S5). Most of them (158 proteins) showed no apparent change in abundance at the proteomic level, suggesting that the transcriptional downregulation was either minor or that these proteins had a low turnover, escaped proteolysis and were kept intact, in spite of their expression down tuning. Some chaperones (e.g., HSP20) are upregulated and could help to

stabilize the proteome during the N stress. The downregulation of 12 transcripts led to a significant decrease in the corresponding proteins:

- three components required for the synthesis of proteins, B7GD73 and B7G7B8 (two translation initiation factor), and B7FUC3 (a Leucyl-Trna synthetase);
- an enzyme involved in the synthesis of photosynthetic membrane lipids, B7G3X5 (plastid monogalactosyldiacylglycerol synthase);
- three enzymes involved in chlorophyll synthesis, B7FWY2 (hydroxymethylbilane synthase), B7G0Z0 (plastid uroporphyrinogen decarboxylase), and B7GDU9 (plastid protoporphyrinogen oxidase);
- a major enzyme of the xanthophyll cycle, B7FYW4 (plastid zeaxanthin epoxidase);

TABLE 2 Analysis of 208 functionally annotated proteins, which abundance was significantly decreased in *P. tricornutum* whole proteome in nitrogen-starved conditions

Annotation cluster 1	Enrichment score: 1.98	Count	P-value
UP sequence feature	DOMAIN:NAD(P)-bd_dom	5	2.4E-3
INTERPRO	NAD(P)-binding domain	5	4.3E-3
COG ontology	Cell envelope biogenesis,outer membrane/carbohydrate transport and metabolism	3	1.1E-1
Annotation cluster 2	Enrichment score: 1.67	Count	P-value
SMART	PINT	3	1.4E-2
UP sequence feature	DOMAIN:PCI	3	2.3E-2
INTERPRO	Proteasome component (PCI)domain	3	3.0E-2
Annotation cluster 3	Enrichment score: 1.6	Count	P-value
GO term "molecular function"	Enzyme regulator activity	3	4.1E-3
UP keyword "cellular component"	Proteasome	4	1.2E-2
GO term "cellular component"	Proteasome complex	3	3.2E-2
KEGG pathway	Proteasome	4	2.4E-1
Annotation cluster 4	Enrichment score: 1.57	Count	P-value
GO term "biological process"	Protoporphyrinogen IX biosynthetic process	4	4.8E-3
KEGG pathway	Porphyrin metabolism	6	5.9E-3
KEGG pathway	Biosynthesis of cofactors	5	6.8E-1
Annotation cluster 5	Enrichment score: 1.47	Count	P-value
INTERPRO	ATP-grasp fold, subdomain 1	3	2.6E-2
INTERPRO	Pre-ATP-grasp domain	3	2.6E-2
UP sequence feature	DOMAIN:ATP-grasp	3	3.9E-2
INTERPRO	ATP-grasp fold	3	5.2E-2
Annotation cluster 6	Enrichment score: 1.41	Count	P-value
KEGG pathway	Histidine metabolism	4	4.4E-3
UP keyword "biological process"	Histidine biosynthesis	3	7.8E-3
GO term "biological process"	Histidine biosynthetic process	3	2.2E-2
UP keyword "biological process"	Amino-acid biosynthesis	4	1.4E-1
KEGG pathway	Biosynthesis of amino acids	4	8.8E-1
Annotation cluster 7	Enrichment score: 1.27	Count	P-value
INTERPRO	Aminoacyl-tRNA synthetase,class 1a, anticodon-binding	4	6.6E-3
INTERPRO	Rossmann-like alpha/beta/alpha sandwich fold	4	1.3E-1
KEGG pathway	Aminoacyl-tRNA biosynthesis	4	1.8E-1
Annotation cluster 8	Enrichment score: 1.14	Count	P-value
UP keyword "domain"	Bromodomain	3	6.1E-2
UP sequence feature	DOMAIN:Bromo	3	7.0E-2
INTERPRO	Bromodomain	3	9.2E-2

Analysis performed as described in Table 1.

- two peroxisomal enzymes, involved either in breaking down fatty acids, B7FXZ0 (acyl-coenzyme A oxidase), or fatty acid conversion into carbohydrates, B7FYT9 (malate synthase);
- two proteins of elusive roles, B7FYU5 and B7FU89.

This proteomic dataset allows, therefore, a refined analysis of the proteome remodeling occurring in diatoms upon nitrogen starvation, and the sophisticated orchestration allowing the selective recycling of nitrogen from proteins without irreversibly affecting cell viability. It is also a resource to identify putative transcription factors, involved in the response to nitrogen scarcity, and controlling the rewiring of diatoms' nitrogen and carbon metabolism. This dataset is also valuable to select gene candidates for future attempts to genetically engineer diatoms for improved biotechnological properties.

ACKNOWLEDGMENTS

J. L. was supported by a PhD grant from a CEA Flagship program. Authors were supported by the French National Research Agency (GRAL Labex ANR-10-LABEX-04, EUR CBS ANR-17-EURE-0003, PROFI ANR-10-INBS-08-01) and IDEX Université Grenoble-Alpes (Glyco@Alps Cross-Disciplinary Program; Grant ANR-15-IDEX-02). Authors thank Khawla Seddiki for technical assistance.

CONFLICT OF INTEREST

The authors declare no conflict of interest.

DATA AVAILABILITY STATEMENT

The proteomics data have been deposited to the ProteomeXchange Consortium via the PRIDE partner repository with the dataset identifier PXD033328.

ORCID

Yohann Couté  <https://orcid.org/0000-0003-3896-6196>

Eric Maréchal  <https://orcid.org/0000-0002-0060-1696>

REFERENCES

1. Benoiston, A. S., Ibarbalz, F. M., Bittner, L., Guidi, L., Jahn, O., Dutkiewicz, S., & Bowler, C. (2017). The evolution of diatoms and their biogeochemical functions. *Philosophical Transactions of the Royal Society of London Series B Biological Sciences*, 1728, 20160397. <https://doi.org/10.1098/rstb.2016.0397>
2. Levitan, O., Dinamarca, J., Hochman, G., & Falkowski, P. G. (2014). Diatoms: a fossil fuel of the future. *Trends in Biotechnology*, 32(3), 117–124. <https://doi.org/10.1016/j.tibtech.2014.01.004>
3. Lupette, J., & Maréchal, E. (2018). Phytoplankton glycerolipids, challenging but promising prospects from biomedicine to green chemistry and biofuels. In S. La Barre & S. S. Bates (Eds.), *Blue Technologies: Production and use of marine molecules* (pp. 191–215). Wiley VCH.
4. Scaife, M. A., & Smith, A. G. (2016). Towards developing algal synthetic biology. *Biochemical Society Transactions*, 44(3), 716–722. <https://doi.org/10.1042/BST20160061>
5. Wang, J. K., & Seibert, M. (2017). Prospects for commercial production of diatoms. *Biotechnology for Biofuels*, 10, 16. <https://doi.org/10.1186/s13068-017-0699-y>
6. Voss, M., Bange, H. W., Dippner, J. W., Middelburg, J. J., Montoya, J. P., & Ward, B. (2013). The marine nitrogen cycle: Recent discoveries, uncertainties and the potential relevance of climate change. *Philosophical Transactions of the Royal Society of London Series B Biological Sciences*, 368(1621), 20130121. <https://doi.org/10.1098/rstb.2013.0121>
7. Bowler, C., Allen, A. E., Badger, J. H., Grimwood, J., Jabbari, K., Kuo, A., Maheswari, U., Martens, C., Maumus, F., Otilar, R. P., Rayko, E., Salamov, A., Vandepoelle, K., Beszteri, B., Gruber, A., Heijde, M., Katinka, M., Mock, T., Valentin, K., ... Grigoriev, I. V. (2008). The Phaeodactylum genome reveals the evolutionary history of diatom genomes. *Nature*, 456(7219), 239–244. <https://doi.org/10.1038/nature07410>
8. Maheswari, U., Mock, T., Armbrust, E. V., & Bowler, C. (2009). Update of the Diatom EST Database: A new tool for digital transcriptomics. *Nucleic Acids Research*, 37, (suppl_1), D1001–D1005. <https://doi.org/10.1093/nar/gkn905>
9. Maheswari, U. (2005). The Diatom EST Database. *Nucleic Acids Research*, 33, (suppl_1), D344–D347. <https://doi.org/10.1093/nar/gki121>
10. Allen, A. E., Laroche, J., Maheswari, U., Lommer, M., Schauer, N., Lopez, P. J., Finazzi, G., Fernie, A. R., & Bowler, C. (2008). Whole-cell response of the pennate diatom Phaeodactylum tricornutum to iron starvation. *Proceedings of the National Academy of Sciences of the United States of America*, 105(30), 10438–10443. <https://doi.org/10.1073/pnas.0711370105>
11. Sapriel, G., Quinet, M., Heijde, M., Jourdain, L., Tanty, V., Luo, G., Le Crom, S., & Lopez, P. J. (2009). Genome-wide transcriptome analyses of silicon metabolism in Phaeodactylum tricornutum reveal the multilevel regulation of silicic acid transporters. *Plos One*, 4(10), e7458. <https://doi.org/10.1371/journal.pone.0007458>
12. Chauton, M. S., Winge, P., Brembu, T., Vadstein, O., & Bones, A. M. (2013). Gene regulation of carbon fixation, storage, and utilization in the diatom Phaeodactylum tricornutum acclimated to light/dark cycles. *Plant Physiology*, 161(2), 1034–1048. <https://doi.org/10.1104/pp.112.206177>
13. Dolch, L.-J., Lupette, J., Tourcier, G., Bedhomme, M., Collin, S., Magneschi, L., Conte, M., Seddiki, K., Richard, C., Corre, E., Fourage, L., Laeuffer, F., Richards, R., Reith, M., Rébeillé, F., Jouhet, J., McGinn, P., & Maréchal, E. (2017). Nitric oxide mediates nitrite-sensing and acclimation and triggers a remodeling of lipids. *Plant Physiology*, 175(3), 1407–1423. <https://doi.org/10.1104/pp.17.01042>
14. Conte, M., Lupette, J., Seddiki, K., Meï, C., Dolch, L.-J., Gros, V., Barette, C., Rébeillé, F., Jouhet, J., & Maréchal, E. (2018). Screening for biologically annotated drugs that trigger triacylglycerol accumulation in the diatom Phaeodactylum. *Plant Physiology*, 532–552. <https://doi.org/10.1104/pp.17.01804>
15. Ait-Mohamed, O., Novák Vanclová, A. M. G., Joli, N., Liang, Y., Zhao, X., Genovesio, A., Tirichine, L., Bowler, C., & Dorrell, R. G. (2020). PhaeoNet: A holistic RNAseq-based portrait of transcriptional coordination in the model diatom Phaeodactylum tricornutum. *Frontiers in Plant Science*, 11, 590949. <https://doi.org/10.3389/fpls.2020.590949>
16. Abida, H., Dolch, L.-J., Meï, C., Villanova, V., Conte, M., Block, M. A., Finazzi, G., Bastien, O., Tirichine, L., Bowler, C., Rébeillé, F., Petroustos, D., Jouhet, J., & Maréchal, E. (2015). Membrane glycerolipid remodeling triggered by nitrogen and phosphorus starvation in Phaeodactylum tricornutum. *Plant Physiology*, 167(1), 118–136. <https://doi.org/10.1104/pp.114.252395>
17. Lupette, J., Jaussaud, A., Vigor, C., Oger, C., Galano, J. - M., Réversat, G., Vercauteren, J., Jouhet, J., Durand, T., & Maréchal, E. (2018). Non-enzymatic synthesis of bioactive isoprostanoïds in the diatom Phaeodactylum following oxidative stress. *Plant Physiology*, 178(3), 1344–1357. <https://doi.org/10.1104/pp.18.00925>
18. Montsant, A., Maheswari, U., Bowler, C., & Lopez, P. J. (2005). Diatoms: Toward diatom functional genomics. *Journal of Nanoscience and Nanotechnology*, 5(1), 5–14.
19. Lupette, J., Jaussaud, A., Seddiki, K., Morabito, C., Brugière, S., Schaller, H., Kuntz, M., Putaux, J. L., Jouneau, P. H., Rébeillé, F., Falconet, D., Couté, Y., Jouhet, J., Tardif, M., Salvaing, J., & Maréchal, E. (2019). The

- architecture of lipid droplets in the diatom *Phaeodactylum tricoratum*. *Algal Research-Biomass Biofuels and Bioproducts*, 38, <https://doi.org/10.1016/j.algal.2019.101415>
20. Wu, S., Gu, W., Jia, S., Wang, L., Wang, L., Liu, X., Zhou, L., Huang, A., & Wang, G. (2021). Proteomic and biochemical responses to different concentrations of CO₂ suggest the existence of multiple carbon metabolism strategies in *Phaeodactylum tricoratum*. *Biotechnology for Biofuels*, 14(1), 235. <https://doi.org/10.1186/s13068-021-02088-5>
21. Chuberre, C., Chan, P., Walet-Balieu, M.-L., Thiébert, F., Burel, C., Hardouin, J., Gügi, B., & Bardor, M. (2022). Comparative proteomic analysis of the diatom *Phaeodactylum tricoratum* reveals new insights into intra- and extra-cellular protein contents of its oval, fusiform, and triradiate morphotypes. *Frontiers in Plant Science*, 13, 673113. <https://doi.org/10.3389/fpls.2022.673113>
22. Leyland, B., Zarka, A., Didi-Cohen, S., Boussiba, S., & Khozin-Goldberg, I. (2020). High resolution proteome of lipid droplets isolated from the pennate diatom *Phaeodactylum tricoratum* (Bacillariophyceae) strain pt4 provides mechanistic insights into complex intracellular coordination during nitrogen deprivation. *Journal of Phycology*, 1642–1663. <https://doi.org/10.1111/jpy.13063>
23. Grouneva, I., Rokka, A., & Aro, E.-M. (2011). The thylakoid membrane proteome of two marine diatoms outlines both diatom-specific and species-specific features of the photosynthetic machinery. *Journal of Proteome Research*, 10(12), 5338–5353. <https://doi.org/10.1021/pr200600f>
24. Alipanah, L., Rohloff, J., Winge, P., Bones, A. M., & Brembu, T. (2015). Whole-cell response to nitrogen deprivation in the diatom *Phaeodactylum tricoratum*. *Journal of Experimental Botany*, 66(20), 6281–6296. <https://doi.org/10.1093/jxb/erv340>
25. Remmers, I. M., D'adamo, S., Martens, D. E., De Vos, R. C. H., Mumm, R., America, A. H. P., Cordewener, J. H. G., Bakker, L. V., Peters, S. A., Wijffels, R. H., & Lamers, P. P. (2018). Orchestration of transcriptome, proteome and metabolome in the diatom *Phaeodactylum tricoratum* during nitrogen limitation. *Algal Research-Biomass Biofuels and Bioproducts*, 35, 33–49. <https://doi.org/10.1016/j.algal.2018.08.012>
26. Longworth, J., Wu, D., Huete-Ortega, M., Wright, P. C., & Vaidyanathan, S. (2016). Proteome response of *Phaeodactylum tricoratum*, during lipid accumulation induced by nitrogen depletion. *Algal Research-Biomass Biofuels and Bioproducts*, 18, 213–224. <https://doi.org/10.1016/j.algal.2016.06.015>
27. Cox, J., & Mann, M. (2008). MaxQuant enables high peptide identification rates, individualized p.p.b.-range mass accuracies and proteome-wide protein quantification. *Nature Biotechnology*, 26, 1367–1372. <https://doi.org/10.1038/nbt.1511>
28. Cunningham, F., Allen, J. E., Allen, J., Alvarez-Jarreta, J., Amode, M. R., Armean, I. M., Austine-Orimoloye, O., Azov, A. G., Barnes, I., Bennett, R., Berry, A., Bhai, J., Bignell, A., Billis, K., Boddu, S., Brooks, L., Charkhchi, M., Cummins, C., Da Rin Fioretto, L., Flicek, P. (2022). Ensembl 2022. *Nucleic Acids Research*, 50(D1), D988–D995. <https://doi.org/10.1093/nar/gkab1049>
29. Wiczorek, S., Combes, F., Borges, H., & Burger, T. (2019). Protein-level statistical analysis of quantitative label-free proteomics data with ProStaR. *Methods in Molecular Biology*, 1959, 225–246. https://doi.org/10.1007/978-1-4939-9164-8_15
30. Schwanhäusser, B., Busse, D., Li, N., Dittmar, G., Schuchhardt, J., Wolf, J., Chen, W., & Selbach, M. (2011). Global quantification of mammalian gene expression control. *Nature*, 473, 337–342. <https://doi.org/10.1038/nature10098>
31. Bateman, A., Martin, M. J., Orchard, S., Magrane, M., Agivetova, R., Ahmad, S., Alpi, E., Bowler-Barnett, E. H., Britto, R., Bursteinas, B., Bye-A-Jee, H., Coetzee, R., Cukura, A., Da Silva, A., Denny, P., Dogan, T., Ebenezer, T., Fan, J., Castro, L. G., ... Teodoro, D. (2021). UniProt: The universal protein knowledgebase in 2021. *Nucleic Acids Research*, 49(D1), D480–D489. <https://doi.org/10.1093/nar/gkaa1100>
32. Huang, D. W., Sherman, B. T., & Lempicki, R. A. (2009). Bioinformatics enrichment tools: Paths toward the comprehensive functional analysis of large gene lists. *Nucleic Acids Research*, 37(1), 1–13. <https://doi.org/10.1093/nar/gkn923>
33. Huang, D. W., Sherman, B. T., & Lempicki, R. A. (2009). Systematic and integrative analysis of large gene lists using DAVID bioinformatics resources. *Nature Protocols*, 4(1), 44–57. <https://doi.org/10.1038/nprot.2008.211>
34. Rosenwasser, S., Graff Van Creveld, S., Schatz, D., Malitsky, S., Tzfadia, O., Aharoni, A., Levin, Y., Gabashvili, A., Feldmesser, E., & Vardi, A. (2014). Mapping the diatom redox-sensitive proteome provides insight into response to nitrogen stress in the marine environment. *Proceedings of the National Academy of Sciences of the United States of America*, 111(7), 2740–2745. <https://doi.org/10.1073/pnas.1319773111>
35. Allen, A. E., Dupont, C. L., Obornik, M., Horák, A., Nunes-Nesi, A., Mccrow, J. P., Zheng, H., Johnson, D. A., Hu, H., Fernie, A. R., & Bowler, C. (2011). Evolution and metabolic significance of the urea cycle in photosynthetic diatoms. *Nature*, 473(7346), 203–207. <https://doi.org/10.1038/nature10074>
36. Kumar Sharma, A., Mühlroth, A., Jouhet, J., Maréchal, E., Alipanah, L., Kissen, R., Brembu, T., Bones, A. M., & Winge, P. (2020). The Myb-like transcription factor phosphorus starvation response (PtPSR) controls conditional P acquisition and remodelling in marine microalgae. *The New Phytologist*, 225(6), 2380–2395. <https://doi.org/10.1111/nph.16248>
37. Smith, R., Jouhet, J., Gandini, C., Nekrasov, V., Marechal, E., Napier, J. A., & Sayanova, O. (2021). Plastidial acyl carrier protein Δ9-desaturase modulates eicosapentaenoic acid biosynthesis and triacylglycerol accumulation in *Phaeodactylum tricoratum*. *Plant Journal*, 106(5), 1247–1259. <https://doi.org/10.1111/tpj.15231>

SUPPORTING INFORMATION

Additional supporting information may be found online <https://doi.org/10.1002/pmic.202200155> in the Supporting Information section at the end of the article.

How to cite this article: Lupette, J., Tardif, M., Brugière, S., Couté, Y., Salvaing, J., & Maréchal, E. (2022). Quantitative proteomic analyses reveal the impact of nitrogen starvation on the proteome of the model diatom *Phaeodactylum tricoratum*. *Proteomics*, 22, e2200155. <https://doi.org/10.1002/pmic.202200155>